

**Argonne National Laboratory**

**KINETICS OF THE REDUCTION  
OF URANIUM OXIDES  
BY CARBON MONOXIDE  
AND BY HYDROGEN**

by

**Milton Volpe**

and

**Slavko Mihailovich**

### LEGAL NOTICE

*This report was prepared as an account of Government sponsored work. Neither the United States, nor the Commission, nor any person acting on behalf of the Commission:*

- A. Makes any warranty or representation, expressed or implied, with respect to the accuracy, completeness, or usefulness of the information contained in this report, or that the use of any information, apparatus, method, or process disclosed in this report may not infringe privately owned rights; or*
- B. Assumes any liabilities with respect to the use of, or for damages resulting from the use of any information, apparatus, method, or process disclosed in this report.*

*As used in the above, "person acting on behalf of the Commission" includes any employee or contractor of the Commission, or employee of such contractor, to the extent that such employee or contractor of the Commission, or employee of such contractor prepares, disseminates, or provides access to, any information pursuant to his employment or contract with the Commission, or his employment with such contractor.*

ARGONNE NATIONAL LABORATORY  
9700 South Cass Avenue  
Argonne, Illinois

KINETICS OF THE REDUCTION OF URANIUM OXIDES BY  
CARBON MONOXIDE AND BY HYDROGEN

by

Milton Volpe and Slavko Mihailovich

Metallurgy Division

Final Report - Program 9.6.1

Partial reports of this work have appeared in sections of the following ANL Metallurgy Division Annual Reports:

<u>Report No.</u>	<u>Pages</u>	<u>Date</u>
ANL-5975	75-76	Dec., 1958
ANL-6099	148-150	Dec., 1959
ANL-6330	244-251	Dec., 1960

July 1962

Operated by The University of Chicago  
under  
Contract W-31-109-eng-38



## TABLE OF CONTENTS

	<u>Page</u>
ABSTRACT . . . . .	4
INTRODUCTION . . . . .	4
EXPERIMENTAL METHODS . . . . .	5
Apparatus . . . . .	5
Materials . . . . .	5
Calibrations . . . . .	7
Procedure During a Run . . . . .	7
Calculations . . . . .	8
Rate Equations . . . . .	8
Thermal Transpiration . . . . .	9
RESULTS . . . . .	11
DISCUSSION . . . . .	15
ACKNOWLEDGMENTS . . . . .	18
REFERENCES . . . . .	19
APPENDIX . . . . .	21



## LIST OF FIGURES

<u>No.</u>	<u>Title</u>	<u>Page</u>
1.	Apparatus . . . . .	6
2.	Effect of Initial Pressure Upon Reaction Rates for Hydrogen and Carbon Monoxide . . . . .	12
3.	Representative Data Plotted as Log P vs t . . . . .	12
4.	Representative Data Plotted as $P^{1/3}$ vs t . . . . .	12
5.	Representative Data Plotted as $P^{1/2}$ vs $t^{1/2}$ . . . . .	13
6.	Reproducibility of Reduction Rate Measurements - $U_3O_8$ at $721^\circ C$ . . . . .	13
7.	Variation of Rate with Oxide Weight - $U_3O_8$ , $H_2$ . . . . .	14
8.	Variation of Rate with Oxide Weight - $U_3O_8$ , $CO$ . . . . .	14
9.	Arrhenius Plot for $H_2$ . . . . .	15
10.	Arrhenius Plot for $CO$ . . . . .	15

## LIST OF TABLES

<u>No.</u>	<u>Title</u>	<u>Page</u>
I.	Activation Energies and Pre-exponential Terms for $CO$ and $H_2$ . . . . .	14
II.	Data for $CO$ . . . . .	21
III.	Data for $H_2$ . . . . .	22



# KINETICS OF THE REDUCTION OF URANIUM OXIDES BY CARBON MONOXIDE AND BY HYDROGEN

by

Milton Volpe and Slavko Mihailovich

## ABSTRACT

The kinetics of the reduction by hydrogen and carbon monoxide of some powdered uranium oxides ( $\text{UO}_{2.1}$ ,  $\text{UO}_{2.2}$ ,  $\text{UO}_{2.4}$ ,  $\text{U}_3\text{O}_8$ ) has been studied by means of a static method. Reductant pressures of about one millimeter of mercury were used, and reaction temperatures ranged from 590 to 950°C. It was found that for all oxide compositions and for reduction by carbon monoxide as well as by hydrogen, the reduction was controlled by a surface process whose rate expression was

$$-dP/dt = \left[ k_0 e^{-E/RT} \right] P^n .$$

The exponent  $n$  was unity for hydrogen and two-thirds for carbon monoxide. The activation energy  $E$  was approximately independent of the nature of the reducing gas. It did depend upon the structure of the oxide, being about 25 kcal/mole for  $\text{U}_3\text{O}_8$  and about 10 kcal/mole for the other compositions.

## INTRODUCTION

In this research, the kinetics of the reduction of uranium oxide powders by carbon monoxide and by hydrogen were investigated in order to determine the mechanism of reduction. Oxides having the nominal compositions  $\text{UO}_{2.1}$ ,  $\text{UO}_{2.2}$ ,  $\text{UO}_{2.4}$ , and  $\text{U}_3\text{O}_8$  were used; initial reductant pressures were about one-half of a millimeter of mercury, and the reaction temperatures were between 590 and 950°C. Although the reduction of  $\text{UO}_3$ ,  $\text{U}_3\text{O}_8$ , and  $\text{U}_4\text{O}_9$  by hydrogen had been studied previously,<sup>(1)</sup> the kinetics of the other interesting phase regions in the uranium dioxide-oxygen system had not been investigated. Furthermore, there had been no references in the literature to any kinetic studies on the reduction of these oxides by carbon monoxide.

In the present research, the "static" method of determining reaction rates was used rather than the more commonly used "dynamic" or flow method. A system of constant volume was used, and the rate of reduction was obtained from measurements of the progressive decrease of gas pressure during reduction. Since small amounts of gas were used, reaction rates were measured without appreciably changing the nominal oxide composition.



The data were used in the usual way<sup>(2)</sup> to obtain rate constants and activation energies for the reduction processes and to obtain information about the reduction mechanism. Most of the effort in this phase of the work was concentrated on finding empirical relationships between pressure and time and comparing them with rate expressions for some plausible mechanisms.

In deriving the rate equations, the usual procedure of postulating the existence of a single, rate-limiting process was followed in order to simplify the mathematics. The various types of rate-limiting processes have been fully discussed in other publications.<sup>(3-6)</sup> Those that have been considered in the present investigation are: (a) the growth of one phase into another; (b) diffusion of oxygen to the surface of the solid (assuming constant surface concentration and semi-infinite boundary conditions); (c) surface adsorption, and (d) surface adsorption followed by diffusion into the solid (assuming a constant concentration gradient).

## EXPERIMENTAL METHODS

### Apparatus

The apparatus used is shown in Figure 1. The high-vacuum furnace was operated through a proportional controller that kept the temperature constant to  $\pm 1^\circ\text{C}$ . The oxide temperature was measured by means of a platinum-10 per cent rhodium thermocouple located within the thin-walled well (B), which terminated less than  $\frac{1}{16}$ -in. from the sample. Pressures were measured by means of a directly heated thermocouple pressure gauge. The control circuit was a new type, which increased the sensitivity and stability of the gauge over those of commercially available units when used in conjunction with a potentiometer-type recorder. The principle of operation involved using a vibrator-type relay to alternately heat the thermocouple and then, by rapidly disconnecting the heater leads while connecting the potentiometer leads, to measure the EMF produced. Because of the rapid make-and-break characteristics of this type of relay, a steady potentiometer reading was obtained, which was accurately a measure of the average heating effect of the pulsating current.

### Materials

#### Gases:

The gases used in this research, hydrogen, carbon monoxide, and oxygen, were all high-purity reagent-grade gases obtained from a commercial supplier in glass bulbs.



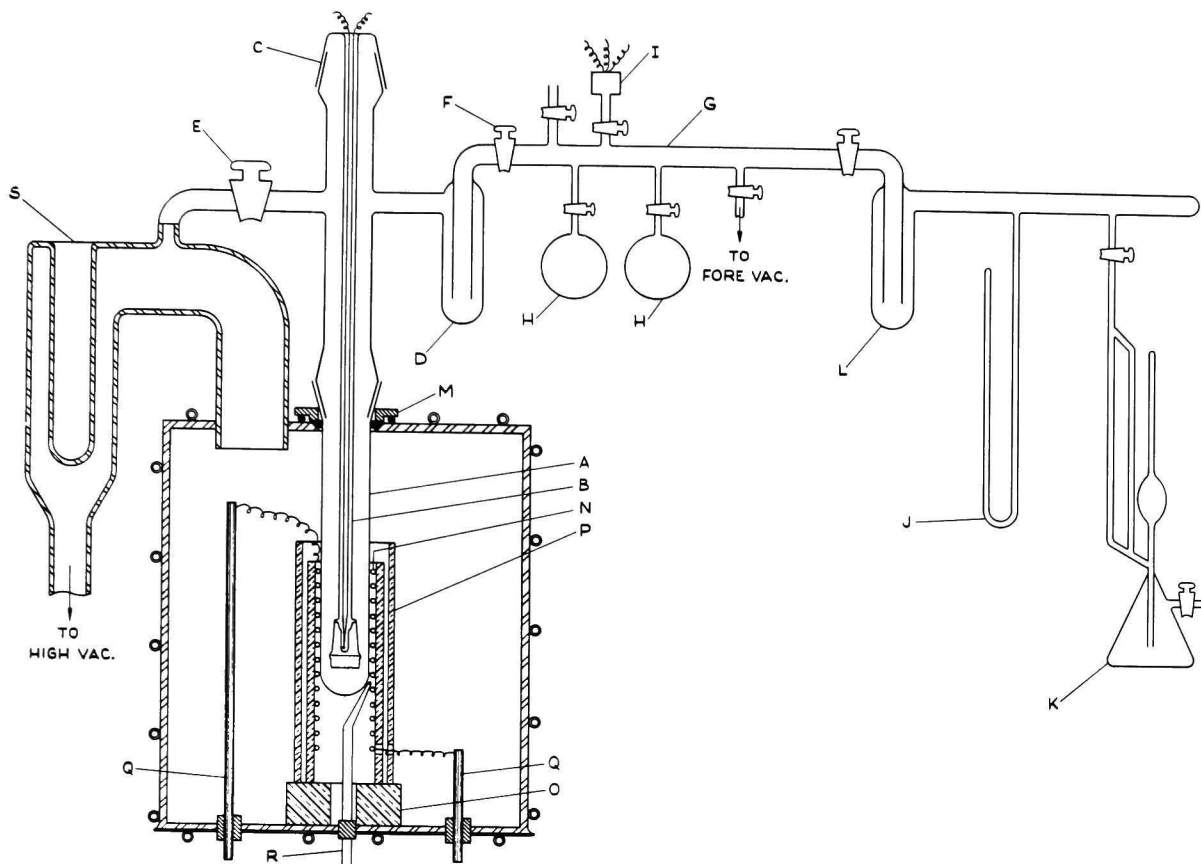


Fig. 1. APPARATUS. (A) is a quartz reaction tube, (B) is a thermocouple tube attached to a Pyrex cap (C). Trap (D) is immersed in liquid nitrogen to a constant height. (E) and (F) are large-bore high-vacuum stopcocks. Attached to the "pipette system" (G) are storage bulbs (H), and a pressure gauge (I). (J) is a mercury manometer and (K) a McLeod pressure gauge. Liquid nitrogen trap (L) serves to prevent contamination by mercury vapor. (M) is an "O"-ring seal that connects the reaction tube to the water-cooled high-vacuum furnace. (N) is a Nichrome heater which rests upon a ceramic pedestal (O) and is surrounded by radiation shields (P). (Q) are current leads and (R) is the control thermocouple. (S) is a liquid nitrogen trap for oil vapors.

#### Oxide Preparation:

$U_3O_8$  powder (surface area =  $0.53 \text{ m}^2/\text{gm}$ ; density ( $CCl_4$ ) =  $8.10 \text{ gm/cc}$ ) was obtained from the air oxidation of chips of high-purity (99.99 per cent) uranium metal. About 50 gm of the oxide were reduced to  $UO_2$  [surface area =  $0.63 \text{ m}^2/\text{gm}$ ; density ( $CCl_4$ ) =  $10.33 \text{ gm/cc}$ ] with hydrogen. This  $UO_2$  was subsequently oxidized to  $UO_{2.1}$ ,  $UO_{2.2}$ ,  $UO_{2.4}$ , and  $U_3O_8$  in the following manner.

The amount of oxygen needed to oxidize a sample of  $UO_2$  to the desired nominal composition was calculated from a knowledge of the sample weight, the system volumes, and the room temperature. This quantity of gas, measured in pipette system (G) (see Figure 1), was allowed to react completely with the  $UO_2$ . X-ray powder patterns indicated that the oxide that resulted from this procedure consisted of  $U_3O_8$  on the surface of the powdered mass and  $UO_2$  within. Therefore, before reduction runs were



made, the heterogeneous oxide was heated in a closed system at 900°C for over 8 hr. X-ray patterns taken after this treatment showed that the composition was then uniform from point to point within the powder. Furthermore, they then showed only cubic-like patterns for all compositions except for  $\text{UO}_{2.4}$ , for which a combination of cubic and hexagonal lines were obtained, and  $\text{U}_3\text{O}_8$ , which gave only hexagonal lines. Although no attempt was made to differentiate between cubic and tetragonal, or between hexagonal and orthorhombic patterns, the X-ray studies gave evidence for the belief that the homogenization procedure produced oxides in their equilibrium phases.<sup>(7)</sup>

In a few cases, the oxide composition was checked by reduction to  $\text{UO}_2$  with carbon monoxide. The resulting carbon dioxide was collected in a liquid nitrogen trap. It was then evaporated into part of the system whose temperature and volume were known, and the pressure was measured. The amount of this carbon dioxide was found to be within 2 per cent of the amount calculated from the composition and weight of the oxide.

### Calibrations

#### Thermocouple Gauge:

Calibration curves were constructed for hydrogen, carbon monoxide, and oxygen by comparing thermocouple gauge readings with McLeod gauge readings for pressures from about one to 900  $\mu$ . The curves were checked from time to time.

#### Apparatus Volumes:

The volumes of the pipette system and other parts of the apparatus were found by expansion of hydrogen from a flask of known volume into the various sections of the apparatus. Pressures of the order of 5 cm of mercury were used so that they could be accurately read on the manometer. For these calibrations, trap (L) was kept at room temperature.

### Procedure during a Run

In making a measurement of a rate of reduction, about one-half gram of the powder was first oxidized to the desired composition. After a period of evacuation at the operating temperature, during which the entire system was pumped down to about  $10^{-5}$  mm Hg, trap (D) (see Figure 1) was immersed in liquid nitrogen to the predetermined level. Stopcock (F) was then closed, and (G) was filled with hydrogen or carbon monoxide to the required pressure. Next, stopcock (E) was closed and (F) opened in order to bring the gas into contact with the oxide. The reaction was allowed to proceed until less than 20  $\mu$  of gas was left (initial pressure was usually about 500  $\mu$ ), and then the residual gas was pumped out. These operations were repeated, resulting in 3 or 4 rate determinations for each set of experimental conditions (composition, temperature, etc.). The last one or two of such a series represented



best the behavior of the system. The decreases in reducible oxygen per run were about 1.5 atomic per cent for  $U_3O_8$  and 10 atomic per cent for  $UO_{2.1}$ . Sometimes (especially when working with  $UO_{2.1}$ ) the oxygen lost in such a series of runs at one temperature was restored before going on to another temperature, but this was not usually done.

### Calculations

In calculating the oxide composition and in converting data from pressure units to molar units, ideal behavior was assumed for all gases. In addition, it was assumed in these calculations that the pressure was uniform throughout the apparatus.

Subject to these assumptions, the oxide composition was calculated from the equation

$$x = 2.34 \times 10^{-3} [PV/gT] \quad . \quad (1)$$

The quantity  $2 + x$  was the O/U ratio of the oxide which was formed by the reaction of  $UO_2$  with oxygen at a pressure of P mm of Hg. In eq. (1), V and T were the volume (in liters) and temperature (in °K) of the pipette system, whereas g was the weight in grams of the  $UO_2$ .

Similarly, the relationship that was used between the molar rate of reaction and the rate expressed as decrease in pressure with time was

$$\begin{aligned} dN/dt &= (N_0/P_0) (dP/dt) \\ N_0 &= (P_1 V/RT) \quad . \end{aligned} \quad (2)$$

Here  $P_0$  is the initial reductant pressure in the reaction tube,  $P_1$  refers to the pressure in the pipette system of volume V, and temperature T is that just before expansion into the reaction tube. In our experiments,  $P_0$  was generally around  $500\mu$ , V was 150 cc, T was 300°K, and  $P_1/P_0$  was 5.18.

### Rate Equations

The experimental rate data were compared with a number of rate equations in order to find the best fit. These equations, together with the mechanisms from which they were derived, were:

(a) If the reduction product formed an adherent layer around the higher oxide and the rate-limiting process was the growth of this outer phase into the other, a "parabolic law" might result.<sup>(4)</sup> In this case, the growth of the outer layer would be given by the equation

$$dx/dt = k'/x \quad , \quad (3)$$



where  $x$  is the thickness of the layer. In the experiments that this report is concerned with, only a thin layer would be formed, so that  $x = k'' (P_0 - P)$ , where  $P_0$  is the initial reductant pressure and  $P$  is the pressure at time  $t$ . When this substitution for  $x$  is made, the result is, after integration,

$$P = P_0 - (Dt)^{1/2} \quad , \quad (4)$$

where  $D$  is a constant. Equation (4) would also result, for the case of thin-film formation, as an approximation to a more complicated one derived by Valensi<sup>(5)</sup> from a mechanism in which diffusion through the product layer would be rate-determining. In addition, the same type of equation could be derived for a diffusion mechanism in which no product layer formed. To do this, semi-infinite boundary conditions (equivalent to the thin layer approximation) would be assumed along with a constant surface concentration.<sup>(8)</sup>

(b) The rate-determining step might have been the adsorption of the reductant on the solid surface or on the solid reactant-product interface. Then, if one assumed again that only a small fraction of the solid were converted, so that the adsorption area could be considered to be constant, the reduction rate would be<sup>(6)</sup>

$$dP/dt = -kP^n \quad , \quad (5)$$

where  $n$  usually would be equal to unity or to  $\frac{1}{2}$ . Equation (5) integrates to give

$$\begin{aligned} \ln P/P_0 &= -kt \quad \text{for } n = 1 \\ P^{(1-n)} &= P_0^{(1-n)} - kt \quad \text{for } n \neq 1 \end{aligned} \quad (6)$$

(c) If surface adsorption and subsequent diffusion into the interior occurred at about equal rates, then, if a constant gradient of diffusing species were assumed, the differential form of the rate equation would be<sup>(6)</sup>

$$dP/dt = \frac{-aP^n}{bP^n + c} \quad . \quad (7)$$

### Thermal Transpiration

To relate pressure to reaction rate, it was necessary to estimate the true pressure at the oxide sample from pressures which were measured at room temperature in another part of the apparatus. In general, because of the effect of thermal transpiration, such pressures differ, the magnitude of their difference being a function of the temperature difference, the gas pressure, and the apparatus dimensions. No data were available for correcting for this effect for temperatures used in this research and so Knudsen's<sup>(9)</sup> formula was used:



$$dP/dT = [P/2T] [1 + 2.46 (r/\lambda)F]^{-2} \quad ,$$

where

$$F = \frac{1 + 3.15 (r/\lambda)}{1 + 24.6 (r/\lambda)} \quad (8)$$

$r$  = radius of reaction tube

$$1/\lambda = 81.1 P(\mu)/T^{1.164} = 81.1 Q_H \text{ for hydrogen}$$

and

$$1/\lambda = 316.2 P(\mu)/T^{1.292} = 316.2 Q_C \text{ for CO} \quad .$$

For both hydrogen and carbon monoxide,  $F$  was found to be essentially constant within limits that were useful in our research, and so equation (8) could be integrated between  $T_2$  and  $T_1$  within those limits. The integrated expression had the form

$$\log(T_1/T_2) = \phi(Q_1) - \phi(Q_2) \quad ,$$

where

$$\phi = [2n(1-2n)]^{-1} \left[ \log_{10} \frac{Q^{4n}}{2n[1+aQ]^2-1} - (2n)^{1/2} \log_{10} \frac{1+aQ-(2n)^{-1/2}}{1+aQ+(2n)^{-1/2}} \right], \quad (9)$$

$a$  and  $n$  being constants which depend on the type of gas. By use of equation (9), curves were made of true reaction tube pressure versus observed thermocouple gauge pressure for each reaction tube temperature.

It is conceded that the use of Knudsen's empirical expression for  $F$  may have been invalid, since it was derived from data that were obtained at temperatures close to room temperature. However, in the absence of thermal transpiration data for temperatures above  $100^\circ\text{C}$ , it, or some other empirical equation<sup>(12)</sup> equally objectionable, had to be used. In a number of cases, rate constants were calculated by means of uncorrected pressures as well as pressures corrected for transpiration. The rate constant differed by about 5%, but the rate expression that was followed remained the same.

An experimental verification of the use of Knudsen's equation was attempted after the reduction experiments were completed. The thermal transpiration effect for both hydrogen and carbon monoxide was measured directly, by means of the so-called "relative" method,<sup>(13)</sup> in a tube whose dimensions approximated those of the reaction tube in the reduction experiment. The experiment was only exploratory; the thermal transpiration



effect was small, and accurate measurements were not possible with the pressure gauges that were used. Nevertheless, the data that were obtained did support the use of Knudsen's equation for the temperatures and thermal gradients that existed in the reduction experiments.

## RESULTS

It was found that for all oxide compositions and for both hydrogen and carbon monoxide, equation (5) with "n" taking a value between unity and two-thirds provided the best fit for the data. Data for hydrogen were plotted (with "n" as unity) according to the integrated equation

$$\log_{10}P = \log_{10}P_0 - (k/2.3)t \quad , \quad (10)$$

whereas for carbon monoxide the equation

$$P^{1/3} = P_0^{1/3} - 1/3kt, \quad (n = 2/3) \quad (11)$$

was used. A list of the observed rates for all of the experiments is given in the Appendix.\* Although these assignments were usually valid, sometimes for the last 10 or 20 per cent of the reaction, a logarithmic plot would give better agreement with carbon monoxide, whereas in others the cube-root plot was best for hydrogen. In a number of cases, the best value for "n" depended on the reaction temperature, so that better agreement with one or the other of the 2 values was obtained as the temperature increased. Such ambiguity was not observed for the first three-quarters of the reaction, and it was from that part of the reaction that rate constants were calculated.

A number of experiments were made to determine whether  $R^*$  was a function of the initial pressure. Figure 2 presents the results of these experiments (with  $U_3O_8$ ) in which only the initial pressure was varied from run to run. Although no effect was observed with hydrogen, with carbon monoxide  $R$  was found to vary with initial pressure, indicating that for it agreement with equation (5) was only approximate. To correct for this pressure effect, all of the  $R$ 's for carbon monoxide were adjusted to a single initial pressure, chosen to be  $600 \mu$ , by use of the data from Figure 2.

---

\*The observed rate constants,  $k$ , are not listed; they were converted by use of equations (2) and (5) into the quantities  $R$ , which are the rates, in units of micromoles per minute, that would have been observed at a reductant pressure of one mm of Hg. Unlike the rate constant, the values of  $R$  are independent of the rate equations used to describe the data; therefore, they permit a more direct comparison to be made between the results for hydrogen and those for carbon monoxide. Like the rate constants, each  $R$  can be factored into a pre-exponential term and an exponential term; the latter contains the activation energy.



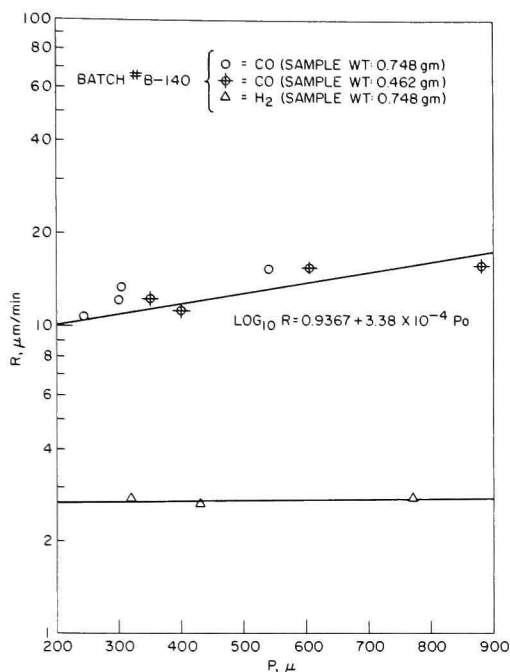


Fig. 2. Effect of Initial Pressure upon Reaction Rates for Hydrogen and Carbon Monoxide

plots such as these, it can be shown that the data do not follow equations (4) or (7).

Although equation (5) was followed for the first part of the reaction, data for the last three-quarters always obeyed the equation

$$P^{1/2} = I - St^{1/2} \quad , \quad (12)$$

which in differential form is

$$\frac{dP}{dt} = \frac{-S^2 P^{1/2}}{I - P^{1/2}} \quad . \quad (13)$$

Figures 3, 4, and 5 provide illustrations of how the data appeared when plotted according to the various kinetic equations. Figure 3 shows that the data for carbon monoxide that are plotted do not agree with equation (10) whereas the data for hydrogen do. In Figure 4, the same data are plotted to show that the carbon monoxide run does follow equation (11) whereas the hydrogen run does not. Figure 5 shows that after a certain "induction period," both sets of data agree with equation (12). By means of

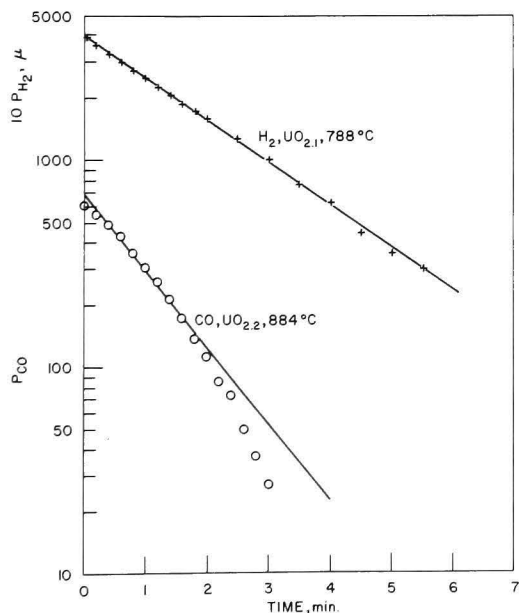


Fig. 3. Representative Data Plotted as  $\text{Log}_{10} P$  vs  $t$

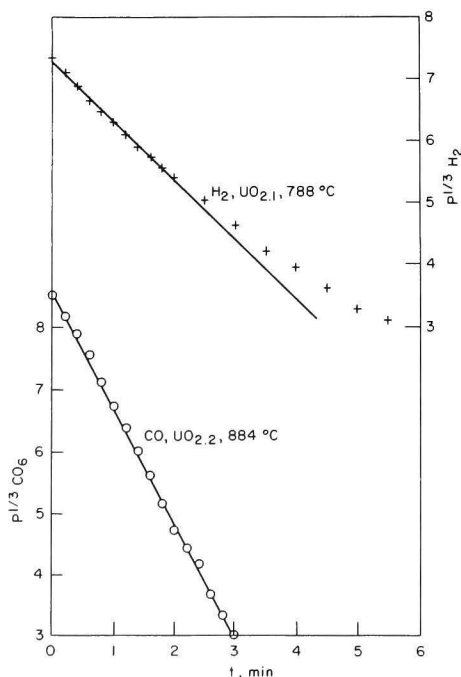


Fig. 4. Representative Data Plotted as  $P^{1/3}$  vs  $t$



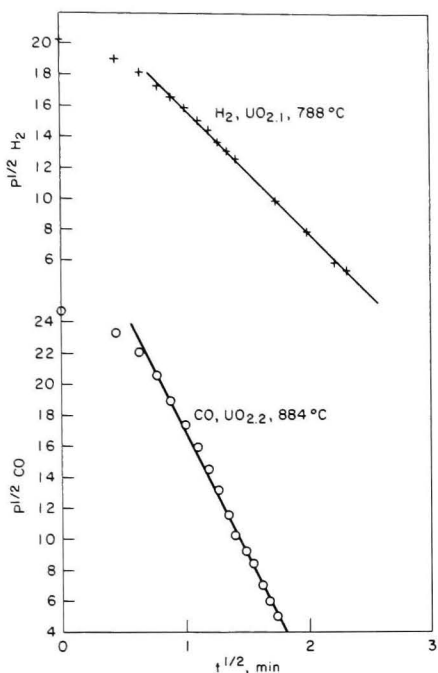


Fig. 5. Representative Data  
Plotted as  $P^{1/2}$  vs  $t^{1/2}$

cent for carbon monoxide and about 2 per cent for hydrogen.

Experiments were carried out with  $U_3O_8$  to determine the effect of sample weight and to determine reproducibility. In this last series, oxide samples were subjected to repeated reduction runs with both hydrogen and carbon monoxide, all made under identical conditions of temperature, pressure, and oxide weight. Typical results of this series are presented in Figure 6, which shows successive runs connected by straight lines. After each group of runs, the oxygen lost by reaction was restored to the oxide. The figure shows clearly that for hydrogen a progressive decrease in rate was obtained, reaching a minimum after about 3 runs, whereas for carbon monoxide the rate increased with number of runs and seemed to level off after 4 or 5 runs. This behavior was not appreciably changed by varying either the oxide batch or the initial gas pressure. This figure shows that the average precision of rate-constant measurements (using the third run) was about 8 per cent for carbon monoxide and about 2 per cent for hydrogen.

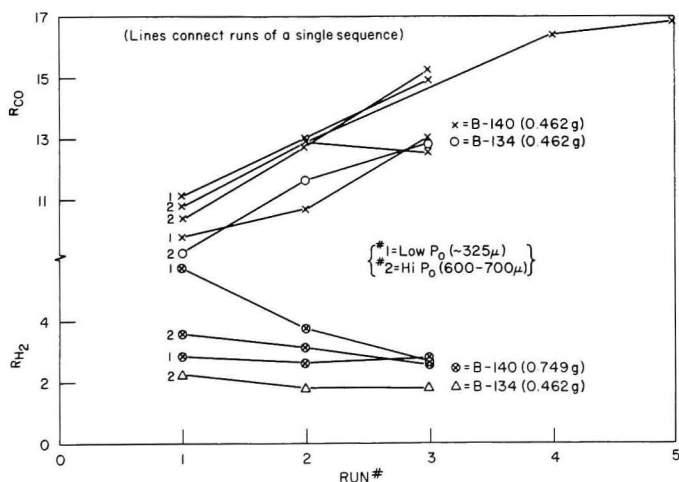


Fig. 6. Reproducibility of Reduction Rate  
Measurements -  $U_3O_8$  at  $721^\circ C$

The effect of oxide weight upon the measured rate is illustrated in Figures 7 and 8. For hydrogen, the rate was found to be approximately proportional to the first power of the weight, whereas for carbon monoxide either a square-root or two-thirds-power dependence was found.



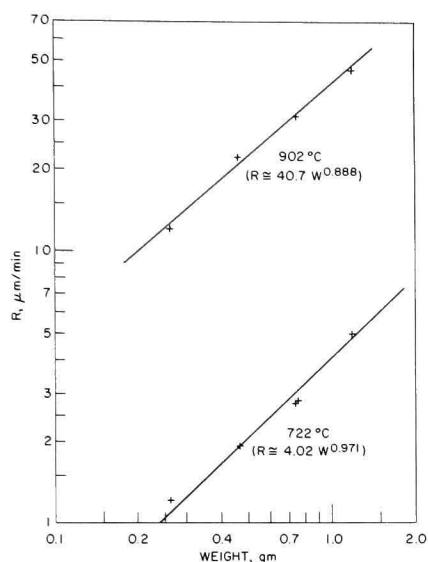


Fig. 7. Variation of Rate with Oxide Weight -  $U_3O_8$  and  $H_2$

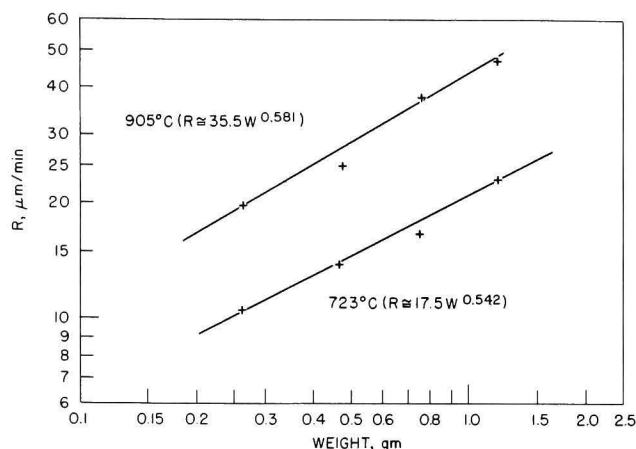


Fig. 8. Variation of Rate with Oxide Weight -  $U_3O_8$  and  $CO$

Activation energies were calculated from rate constants that were obtained from plots for the first two-thirds of the reaction. A list of the activation energies ( $E$ ) and pre-exponential factors ( $R_0$ ) for the various nominal oxide compositions are given in Table I. Figures 9 and 10 are the Arrhenius-law plots from which these activation energies were calculated.\* From these data, 2 conclusions can be drawn immediately. First, the activation energy was nearly the same for reduction by carbon monoxide as for reduction by hydrogen. Secondly, for either gas, the activation energy for  $U_3O_8$  was more than twice the amount of any of the other compositions, each of the latter having about the same activation energy. In addition, (although with less certainty because of the large scatter in the data), it appears from the data that for compositions other than  $U_3O_8$  the magnitudes of both the activation energies and pre-exponential terms decreased slightly with decreasing O/U ratio.

Table I  
ACTIVATION ENERGIES AND PRE-EXPONENTIAL TERMS FOR  $CO$  AND  $H_2$

Composition (nominal)	Hydrogen		Carbon Monoxide	
	$E$ (kcal/mole)	$R_0$ ( $\mu\text{m}/\text{min}$ )	$E$ (kcal/mole)	$R_0$ ( $\mu\text{m}/\text{min}$ )
$U_3O_8$	26.0	$2.0 \times 10^6$	21.1	$3.8 \times 10^5$
$UO_{2.4}$	13.9	$9.6 \times 10^3$	12.9	$5.8 \times 10^3$
$UO_{2.2}$	8.33	$6.2 \times 10^2$	11.7	$3.6 \times 10^3$
$UO_{2.1}$	13.2	$8.9 \times 10^3$	8.50	$7.4 \times 10^2$
Average, Excluding $U_3O_8^*$	11.8	$4.1 \times 10^3$	9.8	$1.5 \times 10^3$

\*From the least-squares straight line fitted to all the points except those for  $U_3O_8$ .

\*For  $U_3O_8$ , the rates plotted in Figures 9 and 10, which correspond to an oxide weight of 0.544 gm, were calculated from observed rates for oxide samples weighing 0.464 gm by use of the data presented in Figures 7 and 8.



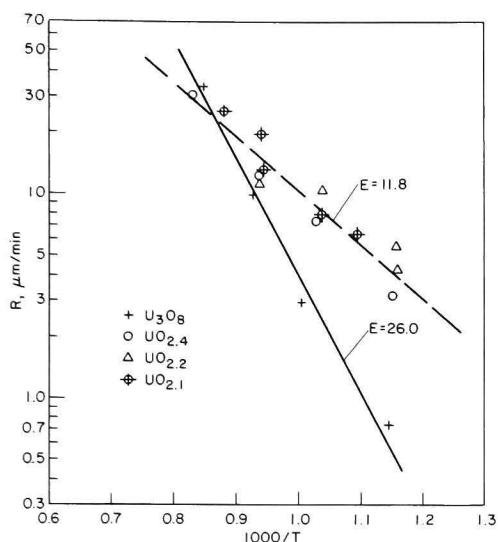


Fig. 9. Arrhenius Plot for  $\text{H}_2$ .  
(Oxide Weight = 0.544 gm)

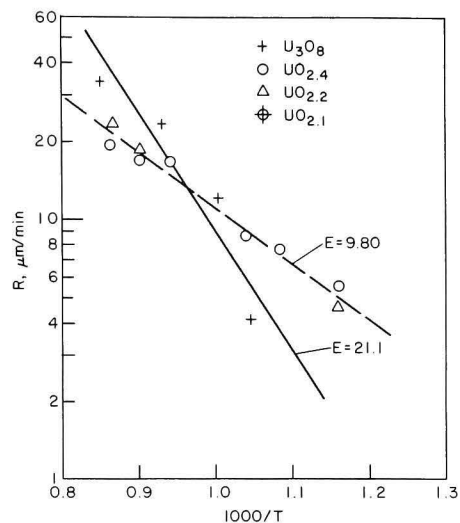


Fig. 10. Arrhenius Plot for  $\text{CO}$ .  
(Oxide Weight = 0.544 gm)

## DISCUSSION

One can conclude from the fact that the data were fitted best by equation (5) that the rate-determining process for reduction by both carbon monoxide and hydrogen was a surface reaction (although for the latter fourth of the reaction some sort of diffusion process may have become dominant). Apparently, reduction with carbon monoxide was much the same as reduction with hydrogen insofar as mechanism, activation energies, pre-exponential factors, and the variation of these quantities with oxide composition were concerned. Evidently, the mechanism for reduction was the same for  $\text{U}_3\text{O}_8$  as for the other oxides, but the activation energies and pre-exponential factors varied with composition.

In spite of the similarity between reduction by carbon monoxide and reduction by hydrogen, it was evident that the data for hydrogen could be interpreted in terms of a simple mechanism with more certainty than could those for carbon monoxide. With hydrogen, after the first few of a series of identical runs, the rate did approach a constant value; the rate was approximately proportional to the first power of the sample weight, and there was no effect of initial pressure on the slope of  $\log P$  versus  $t$  plots. This behavior is what would have been expected if reduction occurred as a single, rate-determining surface reaction. On the other hand, the rate of reduction by carbon monoxide did not approach a constant value after successive runs as readily as it did with hydrogen; it was not proportional to the first power of sample weight, and there was an effect of the initial pressure on the slopes of  $P^{1/3}$  versus  $t$  plots. Thus, it appears as though reduction by carbon monoxide was a more complicated process; perhaps no single rate-determining



step existed. This is in accordance with the findings of Roberts, Walter, and Wheeler.<sup>(10)</sup> Working at temperatures between 400 and 900°C, they found that urania catalyzed the reduction of carbon monoxide to carbon by means of the reaction



The occurrence of this reaction during the reduction of the uranium oxides by carbon monoxide could account for the complex behavior that was observed in the present investigation.

In spite of this, the reduction by both gases can still best be described in terms of a surface-controlled mechanism in which the rate-determining, initial step was the formation of a surface layer of  $\text{UO}_2$  followed by a rapid diffusion of oxygen to the surface. Alternatively, the  $\text{UO}_2$  layer may be imagined to have grown inwards, the rate-determining gas-solid conversion of the higher oxide to  $\text{UO}_2$  taking place at the higher oxide- $\text{UO}_2$  interface. The "interface" mechanism would be equivalent to the "surface" mechanism because the overall oxide composition was maintained approximately constant in the present experiments and only a thin  $\text{UO}_2$  layer formed.

The large difference that was observed in the activation energy for  $\text{U}_3\text{O}_8$  in comparison with the other oxides indicates that the structure of the activated complex for the surface reaction was largely determined by the structure of the oxide being reduced. The formation of the activated complex with  $\text{U}_3\text{O}_8$  would require a greater structural change of the solid than would be required with the cubic and tetragonal oxides. Thus, the  $\text{U}_3\text{O}_8$  activated complex would have the higher energy. The observed similarity in activation energy between hydrogen and carbon monoxide indicates that these structural changes provided a greater contribution to the energy of formation of the activated complex than did the interaction between the gas and the solid. (The oxide  $\text{UO}_{2.4}$  existed in these experiments as a mixture of tetragonal and  $\text{U}_3\text{O}_8$ -like phases. It is reasonable to assume that the reduction of the phase with the lower activation energy, in this case the tetragonal phase, would predominate. This explains why  $\text{UO}_{2.4}$  behaved more like the lower oxides than like  $\text{U}_3\text{O}_8$ .)

Other workers<sup>(1)</sup> who have investigated the hydrogen reduction of  $\text{U}_3\text{O}_8$  and  $\text{U}_4\text{O}_9$  ( $\text{UO}_{2.25}$ ) to  $\text{UO}_2$  have also concluded that a surface process was rate determining. However, the activation energies that they found were generally higher than ours, being 35-26 kcal/mole for  $\text{U}_3\text{O}_8$  and about 26 kcal/mole for  $\text{U}_4\text{O}_9$ . This disagreement may have arisen because of the different experimental techniques that the 2 groups of investigators used.

For instance, our oxide beds were generally thicker than those that the others used (2 mm as opposed to 0.2 mm). Now, Wheeler has shown<sup>(11)</sup> that under certain conditions diffusion of a reactant gas through a solid may be slow enough to affect the rate of reaction of the gas with the solid. In



extreme conditions, the observed activation energy may be one-half of the true energy and the observed pressure dependence may vary considerably from the dependence that would be found if diffusion occurred instantaneously. This may have been the reason for the disagreement in activation energies. In addition, such an effect, being rather sensitive to changes in pore structure, could have caused nonreproducibility in our experiments. The magnitude of this effect was estimated by using the equations given by Wheeler in his paper on reaction rates and selectivity in catalyst pores.<sup>(11)</sup> The pore structure of one  $U_3O_8$  sample was characterized by measuring its surface area, its density in carbon tetrachloride and in mercury, and by microscopic examination. The results of the calculations showed that for the prevailing experimental conditions there should have been no appreciable effects due to gas diffusion. This conclusion held when a single average pore size ( $2\text{-}\mu$  diameter) was assumed or when the powder was assumed to be made up of large-size pores ( $40\text{-}\mu$  diameter), each one being permeated by many small pores ( $2\text{-}\mu$  diameter). Of course, the validity of this conclusion depends upon the accuracy with which the assumed pore structure described the actual one. Moreover, since measurements of pore size were made only with  $U_3O_8$ , it may still have been possible that gas diffusion affected the measurements on the other oxides.

Another possible cause for the disagreement between our activation energies and those of the other workers may be found in the fact that we used a "static" system whereas they (with the exception of Tanford, et al.) used a flow system (weight-loss method). There is good reason to believe that in a static system any effect that gaseous reaction products would have upon the kinetics would be more noticeable than in a flow system. In the former, the reaction products leave the scene of reaction only by diffusion through the reactant gas; in a flow system they are carried away by the gas stream. This effect of the reaction products may have caused the discrepancy in activation energies. In addition, a large part of our experimental error may have been caused by the influence that randomly varying amounts of the reaction products, water and carbon dioxide, had upon our reaction kinetics.

It must also be recognized that the observed rate of decrease of hydrogen or carbon monoxide pressure, which is what was measured in the static method, may not necessarily equal the rate of loss of oxygen from the oxide, which is what the weight-loss method measures. For a simple surface reaction taking place under non-steady-state conditions, the rate of decrease of gas pressure could be greater than the rate of oxygen loss. In this case, the activation energy could be found to be less with the static method than with the weight-loss method. Under steady-state conditions, the 2 rates would be equal and the observed activation energies would be the same for both of the kinetic methods. Insofar as it was possible, we have compared our observed reaction rates with those that were found by the investigators who used the weight-loss method. It



was found that our rates agreed rather well with those of the others, even though their experimental conditions and oxide characteristics were quite different from ours. Therefore, it appears that the lack of agreement in activation energies cannot be ascribed to the absence of steady-state conditions during the reaction. Of course, this point could be definitely cleared up by an experiment in which both weight loss and pressure decrease were measured simultaneously.

In conclusion, the results of this investigation indicate that the reduction of  $\text{UO}_{2.1}$ ,  $\text{UO}_{2.2}$ ,  $\text{UO}_{2.4}$ , and  $\text{U}_3\text{O}_8$  by carbon monoxide and by hydrogen at pressures below one millimeter was predominantly surface controlled. However, there was evidence that the reaction with carbon monoxide was more complex and that the catalytic decomposition of carbon monoxide may have influenced the reduction kinetics. The rate expression that was found to fit the data best for both gases is

$$-dP/dt = \left[ k_0 e^{-E/RT} \right] P^n ,$$

with "n" equal to unity or  $\frac{2}{3}$ . The values of "E" and "k<sub>0</sub>" were about the same for each of the 2 gases; they were not the same for each of the oxides studied, being much larger for  $\text{U}_3\text{O}_8$  than for the other oxides. These differences were interpreted in terms of the structural difference between  $\text{U}_3\text{O}_8$  and the other oxides.

#### ACKNOWLEDGMENTS

The writers wish to express their appreciation to George O'Keefe, who supplied the high-purity  $\text{U}_3\text{O}_8$  samples, and to Drago Kolar, who measured the BET surface areas of some of the oxides. They are also grateful to Ralph Bucknam and William Brookshier of the Electronics Division for modifying the pressure gauge circuit.



## REFERENCES

1. C. W. Kuhlman, Reduction of  $U_3O_8$  with Hydrogen - Reaction Rate, MCW-210 (Aug 19, 1949).  
  
J. Belle and B. Lustman, "Properties of  $UO_2$ ," Fuel Elements Conference, Paris, TID-7546, (March 1958) pp. 442-515.  
  
S. Aronson and J. C. Clayton, Kinetics of the Reduction of  $U_4O_9$  in Hydrogen, J. Inorg. and Nuclear Chem. 7, 384-391 (1958).  
  
C. Tanford, R. L. Tichenor and C. E. Larson, Tuballoy Oxides in the Reduction of  $TO_3$ , AECD-3961 (July 16, 1945).  
  
W. R. DeHollander, A Kinetic Study of the Reduction of Uranium Oxides with Hydrogen, HW-46685 (November 8, 1956).  
  
R. E. DeMarco and M. G. Mendel, The Reduction of High Surface Area Uranium Trioxide, J. Phys. Chem. 6, 132-133 (1959).  
  
U. S. Motz and M. G. Mendel, X-ray and Kinetic Study of the Hydrogen Reduction of  $\gamma-UO_3$ , J. Inorg. and Nuc. Chem. 14, 55-65 (1960).
2. A. A. Frost and R. G. Pearson, Kinetics and Mechanism, J. Wiley and Sons, New York (1958) Ch 1-3.
3. U. R. Evans, "The Mechanism of the Formation of Films on Metals," Pittsburgh Int. Conf. on Surface Reactions, (1948) pp. 71-77.
4. B. Serrin and R. T. Ellickson, Determination of Diffusion Coefficients, J. Chem. Phys. 9, 742-747 (1941).
5. M. G. Valensi, Kinetics of Oxidation of Metallic Spherules and Powders, Compt. rend., 202, 309 (1936).
6. K. J. Laidler, The Mechanism of Some Elementary Surface Reactions, J. Phys. and Coll. Chem., 53, 712-732 (1949).
7. P. E. Blackburn, Oxygen Dissociation Pressures over Uranium Oxides, J. Phys. Chem. 63, 897-902 (1959).
8. J. Crank, The Mathematics of Diffusion, Oxford (1957) Ch. 26.
9. M. Knudsen, Kinetic Theory of Gases, John Wiley and Sons, New York (1952) p. 33.



10. L. E. J. Roberts, A. J. Walter, and V. J. Wheeler, The Oxides of Uranium. Part IX, J. Chem. Soc. (London), 1958, 2472-2481.
11. Ahlborn Wheeler, "Reaction Rates and Selectivity in Catalyst Pores," Advances in Catalysis, III, Academic Press (1951) pp. 250-326.
12. S. Chu Liang, On the Calculation of Thermal Transpiration, Canad. J. Chem. 33, 279-285 (1955).
13. S. Chu Liang, Some Measurements of Thermal Transpiration, J. Appl. Phys. 22, 148-153 (1951).



## APPENDIX

Table II

DATA FOR CO

Oxide O/U Ratio	Oxide Wt(gm)	Run No.	Initial P( $\mu$ )	Temp ( $^{\circ}$ C)	R ( $\mu$ m/min at 1 mm Hg)	R ( $P_0 = 600 \mu$ )
2.40	0.570	3	430	697	6.63	7.57
2.40	0.544	3	450	790	14.7	16.5
2.36	0.544	3	650	889	19.9	19.1
2.27	0.544	3	450	591	4.10	4.61
2.23	0.544	3	430	690	7.34	8.38
2.24	0.544	3	515	838	17.2	18.4
2.25	0.544	3	615	884	23.6	23.3
2.04	0.544	3	460	591	4.98	5.55
2.10	0.544	2	540	691	8.33	8.73
2.08	0.568	3	460	839	15.2	16.9
2.64	0.464	3	465	600	3.37	3.74
2.64	0.464	3	750	721	12.2	10.9
2.64	0.464	3	870	803	26.2	21.2
2.64	0.464	3	490	905	28.0	30.5
2.64	0.462	3	590	720	18.0	18.0
2.64	0.462	3	740	845	28.6	25.6
2.64	0.462	3	475	725	13.3	14.7
2.64	0.462	3	940	846	22.7	17.4
2.64	0.462	3	435	846	24.8	28.2
2.64	1.182	3	508	723	21.6	23.2
2.64	0.748	3	310	723	13.4	16.8
2.64	0.748	3	245	721	10.7	
2.64	0.748	3	300	721	12.1	
2.64	0.748	3	305	721	13.4	
2.64	0.748	3	540	721	15.1	
2.64	0.462	1	346	721	9.15	11.1
2.64	0.462	2	454	721	11.6	13.0
2.64	0.462	3	350	721	12.3	15.0
2.64	0.462	1	324	721	8.71	10.8
2.64	0.462	2	373	721	10.8	12.9
2.64	0.462	3	880	721	15.6	12.6
2.64	0.462	4	650	721	17.1	16.4
2.64	0.462	5	340	721	13.8	16.9
2.64	0.462	1	259	721	7.51	9.79
2.64	0.462	2	360	720	8.88	10.7
2.64	0.462	3	400	720	11.2	13.1
2.64	0.462	1	542	720	9.96	10.4
2.64	0.462	2	530	720	12.1	12.8
2.64	0.462	3	605	720	15.3	15.3
2.64	0.462	1	470	722	8.39	9.28
2.64	0.462	2	390	722	9.88	11.6
2.64	0.462	3	430	722	11.3	12.9
2.64	0.462	3	333	722	11.9	14.6
2.63	0.262	3	340	722	8.48	10.4
2.64	1.182	3	305	902	37.4	47.0
2.64	0.748	3	355	905	31.1	37.6
2.63	0.262	3	360	905	16.4	19.8



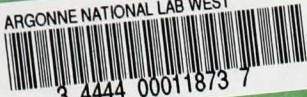
Table III  
DATA FOR H<sub>2</sub>

Oxide O/U Ratio	Oxide Wt (g)	Run No.	Initial P ( $\mu$ )	Temp (°C)	R ( $\mu$ m/min at 1 mm Hg)
2.32	0.544	2	480	595	3.18
2.36	0.544	2	450	698	6.67
2.33	0.544	3	260	698	7.15
2.39	0.544	3	420	792	12.2
2.28	0.544	3	520	928	30.6
2.19	0.544	3	445	590	4.23
2.16	0.544	2	430	592	5.58
2.19	0.544	3	435	690	10.2
2.15	0.544	3	530	792	11.3
2.04	0.544	3	520	641	6.14
2.09	0.544	3	530	690	7.91
2.09	0.544	3	440	786	13.0
2.03	0.544	4	360	786	12.8
2.10	0.544	2	400	788	19.3
2.08	0.544	2	440	860	25.2
2.64	0.464	3	420	601	0.640
2.64	0.464	3	350	721	2.54
2.64	0.464	3	240	803	8.50
2.64	0.464	3	320	905	28.4
2.64	0.462	3	350	720	2.66
2.64	0.462	3	360	845	17.7
2.64	0.462	3	330	721	2.00
2.64	0.462	3	370	845	13.0
2.64	1.182	3	432	723	4.90
2.64	0.748	1	550	722	2.83
2.64	0.748	2	530	722	2.65
2.64	0.748	3	770	722	2.80
2.64	0.748	1	340	722	5.79
2.64	0.748	2	260	722	3.80
2.64	0.747	3	430	722	2.68
2.64	0.748	1	330	722	3.60
2.64	0.748	2	285	722	3.18
2.64	0.748	3	320	720	2.74
2.64	0.462	3	700	721	1.93
2.64	0.462	1	470	721	2.29
2.64	0.462	2	495	721	1.92
2.64	0.462	3	305	721	1.89
2.63	0.262	3	300	721	1.21
2.64	1.182	3	425	903	45.7
2.64	0.748	3	472	905	31.0
2.64	0.462	3	380	905	22.0
2.63	0.262	3	420	904	12.0



X<sup>2</sup>

ARGONNE NATIONAL LAB WEST



3 4444 00011873 7

